

TABLE 6.1a SUMMARY OF THRESHOLD DETECTION PARAMETERS: "ON-OFF" INPUT SIGNALS*

"On-off" Input Signals	Coherent Threshold Detection		Incoherent Threshold Detection	
	Optimum	Cross-correlator	Optimum	Auto-correlator
$\sigma_0^{(*)2}$	$L \sum_i \langle a_{oi} s_i \rangle^2$ $\rightarrow nL \bar{a}_0^2$ <p>[Eq. (6.9); Eq. (A.2-14).]</p>	$\sum_i \langle a_{oi} s_i \rangle^2 \rightarrow n \bar{a}_0^2$ <p>[Eqs. (6.16), (A.4-8).]</p>	$\frac{1}{4} \sum_{ij} \langle a_{oi} a_{oj} s_i s_j \rangle^2 \{2L(2)^2 + [L(4) - 2L(2)] \delta_{ij}\}$ <p>[Eqs. (6.22a), (A.2-40)]</p>	$\left(\sum_{ij} \langle a_{oi} a_{oj} s_i s_j \rangle^2 \right)^2$ $\sum_{ij} \langle a_{oi} a_{oj} s_i s_j \rangle^2 (x-3) \delta_{ij+2}$ <p>[Eqs. (6.35), (A.4-16)]</p>
$\langle a_0^2 \rangle^{(*)}$ min-()	$\frac{1}{2n} \sum_i \langle a_{oi} s_i \rangle^2$ $\rightarrow \bar{a}_0^2$	<p>=(same); Eq. (6.17)</p>	$\frac{1}{n} \sum_i \langle a_{oi} s_i \rangle^2 \rightarrow \bar{a}_0^2$	<p>=(same); Eq. (6.36)</p>
<u>minimum detectable signal</u>	$= (\pi_{coh}^*)^{-1} (C_{N.P.}^*)$ <p>or $C_{I.O.}^*)^2$</p> <p>Eqs. (6.10), (6.11)</p>	$= \pi_{coh}^{-1} (C_{N.P.} \text{ or } C_{I.O.})^2$ <p>Eqs. (6.17); (6.21a)</p>	$= (\pi_{inc}^*)^{-1/2} (C_{N.P.} \text{ or } C_{I.O.})$	$= \pi_{inc}^{-1/2} (C_{N.P.} \text{ or } C_{I.O.})$ <p>Eq. (6.37)</p>

* See "Notes", p. 73.

TABLE 6.1a. (Cont'd.)

"On-off" Input Signals	Coherent Threshold Detection		Incoherent Threshold Detection	
	Optimum	Cross-correlator	Optimum	Auto-correlator
$\Pi \begin{pmatrix} * \\ \end{pmatrix}$	$nL(2);$ Eq. (6.10)	n Eq. (6.17).	$\frac{nL(4)}{8} \left[1 + \frac{2L(2)^2}{L(4)} (Q_n - 1) \right];$ Eq. (6.24)	$\frac{nQ_n^2}{2[(x^4 - 1) + 2(Q_n - 1)]}$ Eq. (6.36)
<u>Processing gain</u>			$Q_n - 1 = \frac{1}{n} \sum_{ij} m_{ij}^2 \rho_{ij}^2 (\geq 1)$ Eq. (6.25).	
$\Phi_d^* ()$ Degradation Factor	1	$1/L(2);$ Eq. (6.18)	1	$4Q_n^2 / L(4) \left(1 + \frac{2L(2)^2}{L(4)} Q_n - 1 \right)$ $\cdot [(x^4 - 1) + 2(Q_n - 1)],$ Eq. (6.38).
$\hat{B}_{inc} \begin{pmatrix} * \\ \end{pmatrix};$ Bias Terms	$-\sigma_{0-coh}^{(*)2} / 2$	Eq. (A.4-55)	$-\sigma_{0-inc}^{(*)2} / 2$	Eq. (A.4-55)

TABLE 6.1a (Cont'd.)

* NOTES: (i). $C_{N.P.}^{(*)} \equiv \theta^{-1} (2p_D^{(*)} - 1) + \theta^{-1} (1 - 2\alpha_F^{(*)})$; $C_{I.O.}^{(*)} \equiv 2\theta^{-1} (1 - 2p_e^{(*)})$; Eq. (6.11)

with $p_D^{(*)} \equiv P_D^{(*)}/p$;

- (ii). Stationary noise; independent noise samples (n) ; symmetrical pdf's of the instantaneous noise amplitudes (x) ;
- (iii). Data acquisition period $(\sim n)$ is large, so that the various detection algorithms, $g\{\}$, are asymptotically normal under H_0, H_1 .
- (iv). The LOBD's here (i.e. "optimum algorithms") are AODA's as well. The generally suboptimum correlation detectors are optimum only in gauss noise. [See Appendix A.3.]
- (v). For signals with incoherent structure, $Q_n \approx 1$. For signals with completely coherent structure, $Q_n \sim 0(n)$; in particular, for sinusoidal wave trains, $Q_n \approx n/2$, cf. (A.2-42e).

TABLE 6.1b. SUMMARY OF THRESHOLD DETECTION PARAMETERS:

I. Binary Input Signals: $\sigma_{0-}^{(21)(*)2}$

Coherent Threshold Detection		Incoherent Threshold Detection	
Optimum	Cross-correlator	Optimum	Auto-correlator
$L^{(2)} \sum_i^n \{ \langle a_{oi}^{(2)} s_i^{(2)} \rangle - \langle a_{oi}^{(1)} s_i^{(1)} \rangle \}^2 - \langle a_{oi}^{(1)} s_i^{(1)} \rangle^2$	$\sum_i^n \{ \langle a_{oi}^{(2)} s_i^{(2)} \rangle - \langle a_{oi}^{(1)} s_i^{(1)} \rangle \}^2$	$\frac{1}{4} \sum_{ij}^n \{ \langle a_{oi}^{(2)} a_{oj}^{(2)} s_i^{(2)} s_j^{(2)} \rangle - \langle a_{oi}^{(1)} a_{oj}^{(1)} s_i^{(1)} s_j^{(1)} \rangle \}^2$	$\frac{a_0^{(2)} \neq a_0^{(1)}}{(\langle a_0^{(2)} \rangle - \langle a_0^{(1)} \rangle)^2 n Q_n^{(21)2}}$
$a_0^{(2)} = a_0^{(1)}$	$\bar{a}_0^2 \sum_i \{ \langle s_i^{(2)} \rangle - \langle s_i^{(1)} \rangle \}^2$	$\cdot \{ (L^{(4)} - 2L^{(2)2}) \delta_{ij} + 2L^{(2)2} \}$	$\frac{(\bar{x}^4 - 1) + 2(Q_n^{(21)})^2 - 1}{(x^4 - 1) + 2(Q_n^{(21)})^2 - 1}$
$L^{(2)} \bar{a}_0^2 \sum_i \{ \langle s_i^{(2)} \rangle - \langle s_i^{(1)} \rangle \}^2$	$\bar{a}_0^2 \sum_i \{ \langle s_i^{(2)} \rangle - \langle s_i^{(1)} \rangle \}^2$	$\frac{a_0^{(2)} = a_0^{(1)}}{\frac{\bar{a}_0^2 L^{(2)2}}{2} \sum_{ij}^n \langle s_i^{(1)} s_j^{(1)} \rangle^2 (\rho_{ij}^{(2s)})}$	$a_0^{(2)} = a_0^{(1)}$
$[Eq. (6.12)]$	$[Eqs. (6.19), (6.20)]$	$- \rho_{ij}^{(1s)} \}^2 [Eqs. (6.28), (6.33)].$	$\text{same as above; } Q_n^{(21)} \rightarrow Q_n^{(21)}$
			$[Eq. (6.41)]$

TABLE 6.1b. SUMMARY OF THRESHOLD DETECTION PARAMETERS:

II. Binary Input Signals: $\langle a_0^{(2)} \rangle_{\min}^{(21)*}$

Coherent Threshold Detection		Incoherent Threshold Detection	
Optimum	Cross-Correlator	Optimum	Auto-correlator
$\frac{1}{2n} \sum_i \{ \langle a_{oi}^{(2)} s_i^{(2)} \rangle - \langle a_{oi}^{(1)} s_i^{(1)} \rangle \}^2$ <p>[Eq. (6.13)].</p>	<p>→ same, cf. Eq. (6.19)</p>	$\frac{1}{n} \sum_i \{ \langle (a_{oi}^{(2)} s_i^{(2)})^2 \rangle - \langle (a_{oi}^{(1)} s_i^{(1)})^2 \rangle \}^2$ $= \langle a_0^{(2)} \rangle^2 - \langle a_0^{(1)} \rangle^2;$ <p>$(a_0^{(2)} \neq a_0^{(1)}),$ [Eq. (6.29)]</p>	<p>same; Eq. (6.39a).</p>
$\bar{a}_0^{(2)} = a_0^{(2)} : \rightarrow \frac{1}{2n} \sum_i \{ \langle s_i^{(2)} \rangle - \langle s_i^{(1)} \rangle \}^2$ <p>Eq. (6.14).</p>	<p>→ same, cf. Eq. (6.20).</p>	<p>→ $\bar{a}_0^{(2)} : (a_0^{(1)} = a_0^{(2)})$.</p> <p>Eq. (6.33)</p>	<p>→ same; Eq. (6.41)</p>
$= (\pi_{\text{coh}}^{(21)*})^{-1} (C_{\text{N.P. or } C_{\text{I.O.}}}^*)^2$ <p>[Eq. (6.13a)].</p>	$= \pi_{\text{coh}}^{(21)-1} (C_{\text{N.P. or } C_{\text{I.O.}}})^2$ <p>[Eq. (6.13a)]</p>	$= (\pi_{\text{inc}}^{(21)*})^{-1/2} (C_{\text{N.P. or } C_{\text{I.O.}}}^*)^{-1/2}$ <p>[Eq. (6.34)]</p>	$= (\pi_{\text{inc}}^{(21)})^{-1/2} (C_{\text{N.P. or } C_{\text{I.O.}}})^{-1/2}$ <p>[Eq. (6.37)]</p>

TABLE 6.1b. SUMMARY OF THRESHOLD DETECTION PARAMETERS
 III. Binary Input Signals: $\pi^{(21)*}$: Processing Gain

Coherent Threshold Detection		Incoherent Threshold Detection	
Optimum	Cross-correlator	Optimum	Auto-correlator
$n_L^{(2)}$ [Eq. (6.10)]	n [Eq. (6.20)]	$a_0^{(1)} = a_0^{(2)}$: $\frac{n_L^{(2)2}}{4} \sum_{ij} m_{ij}^{(2s)} \frac{m_{ij}^{(2s)}}{n^2 \rho_{ij}} - \rho_{ij}^{(1s)2} = \frac{n_L^{(2)2}}{4} (\hat{Q}_n^{(21)} - 1)$ [Eq. (6.33), (6.33a)]	$n Q_n^{(21)2} / 2[(x_n^2 - 1) + 2(Q_n^{(21)} - 1)]$ $a_0^{(1)} \neq a_0^{(2)}$: [Eq. (6.40)]
		$a_0^{(1)} \neq a_0^{(2)}$: $\frac{n_L^{(4)} \{1 + \frac{2L^{(2)2}}{L} (Q_n^{(21)} - 1)\}}{8}$ [Eq. (6.30), see Eq.(6.31) for $Q_n^{(21)}$]	[Eq. (6.41)]: $a_1^{(1)} = a_0^{(2)}$: $\frac{n(\hat{Q}_n^{(12)} - 1)^2}{2[(x_n^2 - 1) + 2(\hat{Q}_n^{(21)} - 1)]}$

TABLE 6.1b. SUMMARY OF THRESHOLD DETECTION PARAMETERS:

IV. Binary Input Signals: $\phi_{d-}^{(21)*}$, Degradation Factor

Coherent Threshold Detection		Incoherent Threshold Detection	
1	$1/L^{(2)}$, Eq. (6.2)	1	Eq. (6.42a): $a_0^{(1)} \neq a_0^{(2)}$ Eq. (6.42b): $a_0^{(1)} = a_0^{(2)}$

V. Binary Input Signals: $\hat{B}_n^{(*)}$: Bias

$-\frac{L^{(2)}}{2} \sum_i \langle (a_{0i}^{(2)} s_i^{(2)})^2 \rangle$	$-\frac{1}{2} \sum_i \langle (a_{0i}^{(2)} s_i^{(2)})^2 \rangle$	$-\frac{1}{8} \sum_{ij} \langle (a_{0i}^{(2)} a_{0j}^{(2)} s_i^{(2)} s_j^{(2)})^2 \rangle$	$-\frac{1}{2} \sum_i \langle (a_{0i}^{(2)} s_i^{(2)})^2 \rangle$
$-\langle a_{0i}^{(1)} s_i^{(1)} \rangle^2$	$-\langle a_{0i}^{(1)} s_i^{(1)} \rangle^2$;	$-\langle a_{0i}^{(1)} a_{0j}^{(1)} s_i^{(1)} s_j^{(1)} \rangle^2$	$-\langle (a_{0i}^{(1)} s_i^{(1)})^2 \rangle \frac{1}{4} \sum_{ij}$
[Eq. (4.3a)]	[Eq. (4.9)]	$\cdot \langle (L^{-2} \sum_{ij} \delta_{ij} + 2L^{(2)})^2 \rangle$	$\cdot \langle (a_{0i}^{(2)} a_{0j}^{(2)} s_i^{(2)} s_j^{(2)})^2 \rangle$
		[Eqs. (4.5a), (A.2-52b)]	$-\langle a_{0i}^{(1)} a_{0j}^{(1)} s_i^{(1)} s_j^{(1)} \rangle^2$
			[Eq. (4.12b)]

TABLE 6.2 THRESHOLD DETECTION PARAMETERS: (SUBOPTIMUM) CLIPPER-CORRELATORS

I. Detector Structure: $g(\underline{x})$

Coherent Threshold Detection		Incoherent Threshold Detection	
"On-Off" Signals	Binary Signals	"On-Off" Signals	Binary Signals
$\log \mu + \hat{B}_{coh}^i + \sqrt{2} \sum_i^N \langle \theta_i \rangle$ $\cdot \text{sgn } x_i$ $[\theta_i = a_{oi} s_i]$	$\log \mu + \hat{B}_{coh}^i + \sqrt{2} \sum_i^N \langle \theta_i \rangle$ $\cdot (\langle \theta_i^{(2)} \rangle - \langle \theta_i^{(1)} \rangle) \text{sgn } x_i$	$\log \mu + \hat{B}_{inc}^i + \sum_{ij} \langle \theta_i \theta_j \rangle \text{sgn } x_i$ $\cdot \text{sgn } x_j$	$\log \mu + \hat{B}_{inc}^{(21)} + \sum_{ij} \Delta \rho_{ij}^{(21)} \text{sgn } x_i$ $\Delta \rho_{ij}^{(21)} = \text{Eq. (2.13a)}$

II. Detector Variances: $\hat{\sigma}_0^2$

$2 \sum_i^N \langle \theta_i \rangle^2$ <p>Eq. (A.4-68)</p>	$2 \sum_i^N \{ \langle \theta_i^{(2)} \rangle^2 - \langle \theta_i^{(1)} \rangle^2 \}$ <p>Eq. (A.4-73)</p>	$\sum_{ij}^N \langle \theta_i \theta_j \rangle^2 (2 - \delta_{ij})$ <p>Eq. (A.4-68)</p>	$\sum_{ij}^N [\langle \theta_i \theta_j \rangle^{(2)} - \langle \theta_i \theta_j \rangle^{(1)}]^2$ $\cdot (2 - \delta_{ij});$ <p>Eq. (A.4-73)</p>
---	--	---	--

TABLE 6.2 THRESHOLD DETECTION PARAMETERS: (SUBOPTIMUM) CLIPPER-CORRELATORS

III. Detector Variances: σ_0^2

Coherent Threshold Detection		Incoherent Threshold Detection	
"On-Off" Signals	Binary Signals	"On-Off" Signals	Binary Signals
$4w_{1E}(0)^2 \sum_i^n \langle \theta_i \rangle^2$ Eq. (A.4-69a)	$4w_{1E}(0)^2 \sum_i^n (\langle \theta_i^{(2)} \rangle - \langle \theta_i^{(1)} \rangle)^2$ Eq. (A.4-74a)	$(\sum_{ij} \langle \theta_i \theta_j \rangle^2 \{8w_{1E}(0)^2 (1-\delta_{ij}) - \sqrt{2}w_{1E}''(0) \delta_{ij}\})^2$ $4 \sum_{ij} \langle \theta_i \theta_j \rangle^2 (2-\delta_{ij})$ Eq. (A.4-69b)	→ same with $\langle \theta_i \theta_j \rangle^2 \rightarrow (\langle \theta_i \theta_j \rangle^{(2)})^2 - (\langle \theta_i \theta_j \rangle^{(1)})^2$ Eq. (A.4-74b)

IV. Minimum Detectable Signal: $a_0^2 \min(-)$

\bar{a}_0^2 $\Pi_{coh}^{-1} (C_{N.P. or C_{I.O.}})^2$	$\left\{ \frac{1}{2n} \sum_i^n [(\overline{a_{oi} s_i})^{(2)} - (\overline{a_{oi} s_i})^{(1)}]^2 \right\}$ $\Pi_{coh}^{(21)-1} (C_{N.P. or C_{I.O.}})^2$	\bar{a}_0^2 $\Pi_{inc}^{-1/2} (C_{N.P. or C_{I.O.}})$	$\left\{ \frac{1}{n} \sum_i^n [(\langle \theta_i^{(2)} \rangle - \langle \theta_i^{(1)} \rangle)^2]^2 \right\}^{1/2}$ $(\Pi_{inc}^{(21)})^{-1/2} (C_{N.P. or C_{I.O.}})$
--	---	--	---

TABLE 6.2 THRESHOLD DETECTION PARAMETERS: (SUBOPTIMUM) CLIPPER CORRELATORS

V. II { }, Processing Gain

Coherent Threshold Detection		Incoherent Threshold Detection	
"On-off" Signals	Binary Signals	"On-off" Signals	Binary Signals
$4w_{1E}(0)^2 n$	$4w_{1E}(0)^2 n$	$\frac{\left(\sum_{ij} m_{ij}^2 \rho_{ij}^2 \{ 8w_{1E}(0)^2 (1-\delta_{ij}) - \sqrt{2} w_{1E}''(0) \delta_{ij} \} \right)^2}{8 \sum_{ij} m_{ij}^2 \rho_{ij}^2 (2-\delta_{ij})}$	$\left. \begin{aligned} &(a_{01} \neq a_{02}): \\ &\text{same:} \\ &\rho_{ij} \rightarrow \rho_{ij} \begin{matrix} (2) \\ (1) \end{matrix} - \rho_{ij} \end{aligned} \right\}$
		$= \frac{n[-\sqrt{2} w_{1E}''(0) + 8w_{1E}(0)^2 \cdot (Q_n - 1)]^2}{8(2Q_n - 1)}$	$\frac{n[-\sqrt{2} w_{1E}''(0) + 8w_{1E}(0)^2 \cdot (Q_n^{(21)} - 1)]^2}{8(2Q_n^{(21)} - 1)}$
			$\frac{a_{01} = a_{02}:}{8n [w_{1E}(0)^4 (\hat{Q}_n^{(21)} - 1)]}$
			$Q_n \rightarrow \hat{Q}_n^{(21)}$

TABLE 6.2 THRESHOLD DETECTION PARAMETERS: (SUBOPTIMUM) CLIPPER CORRELATORS

VI. Detector Structure: $\Phi_{d-}^*(\cdot) (\equiv \Pi(\cdot) / \Pi^*(\cdot))$, Degradation Factor

Coherent Threshold Detection		Incoherent Threshold Detection	
"On-Off" Signals	Binary Signals	"On-Off" Signals	Binary Signals
$\frac{4w_{1E}(0)^2}{L_E^{(2)}}$	$\frac{4w_{1E}(0)^2}{L_E^{(2)}}$	$\frac{[-\sqrt{2}w_{1E}''(0) + 8w_{1E}(0)^2(Q_n - 1)]^2}{L^{(4)}(1 + \frac{2L^{(2)}}{4})[Q_n - 1][1 + 2(Q_n - 1)]}$	$\left\{ \begin{array}{l} (a_{01} = a_{02} = a_0): \\ \rho_{ij} \rightarrow \rho_{ij}^{(2)} - \rho_{ij}^{(1)} \\ Q_n \rightarrow Q_n^{(21)} \end{array} \right.$
		$[=1: F \rightarrow E; (A.4-36) - (A.4-46)]$	$F \rightarrow E: = 1$
		in (A.4-31)	

VII. Detector Structure: Bias: $\hat{B}_i^i(\cdot)$

$-2\sqrt{2}w_1(0) \sum_i^n \bar{a}_{0i}^2$	$-\sqrt{2}w_{1E}(0)\bar{a}_0^2$	$-(1 - \sqrt{2}w_{1E}(0)) \sum_i^n \langle \theta_i^2 \rangle$	same:
$= -2\sqrt{2} \bar{a}_0^2 w_{1E}(0)n$	$\cdot \sum_i^n (\langle s_i^{(2)} \rangle - \langle s_i^{(1)} \rangle)^2$	$-\frac{1}{4} \sum_{ij}^n \langle \theta_i \theta_j \rangle^2 \{ 8w_{1E}(0)^2$	$\langle \theta_i^2 \rangle \rightarrow \Delta \rho_{ij}^{(21)}$
Eq. (A.4-66a)		$\cdot (1 - \delta_{ij})^{-\delta_{ij}} \sqrt{2}w_{1E}''(0) \}$	$\langle \theta_i \theta_j \rangle = \Delta \rho_{ij}^{(21)}$, etc.
		Eq. (A.4-66b).	

TABLE 6.2 THRESHOLD DETECTION PARAMETERS: (SUBOPTIMUM) CLIPPER CORRELATORS

(Cont'd.)

NOTES: 1). Stationary noise régimes

2). When $F \rightarrow E$: the detectors are "matched" to the noise, i.e. are now (threshold) optimum for the Class E pdf $w_{1E}(x)_0$, we must use the optimum (LOBD) results of Tables (6.1a,b).

$$3). Q_{n-1} \equiv \frac{1}{n} \sum_{ij}^{n'} m_{ij}^2 \rho_{ij}^2 (\geq 0); \quad Q_{n-1}^{(21)} = \frac{1}{n} \sum_{ij}^{n'} m_{ij}^2 (\rho_{ij}^{(2)} - \rho_{ij}^{(1)})^2; \quad (a_0^{(2)} = a_0^{(1)} = a_0).$$

V. General Remarks:

From the results above we can make the following general observations:

- (i). Processing gain for coherent threshold reception ($\Pi_{\text{coh}}^{(*)}$, LOBD or cross-correlator) is proportional to sample size (or observation time), i.e.,

$$\Pi_{\text{coh}}^{(*)} \sim n ; [\text{Eqs. (6.10), (6.13), (6.17), (6.20)}]. \quad (6.43a)$$

- (ii). Processing gain for incoherent threshold reception ($\Pi_{\text{inc}}^{(*)}$, LOBD or auto-correlator), on the other hand, is $\sim (n^\mu)$, $1 \leq \mu \leq 2$, e.g.:

$$\Pi_{\text{inc}}^{(*)} \sim n^\mu, \quad 1 \leq \mu \leq 2: [\text{Eqs. (6.24), (6.25); (6.30), (6.31); (6.33), (6.36b), (6.41)}]. \quad (6.43b)$$

If the received signal is sufficiently decorrelated that

$$Q_n^{-1} \equiv \frac{1}{n} \sum_{ij} m_{ij}^2 \rho_{ij}^2,$$

cf. (6.25) for example, is $O(n^0)$, i.e. at most there are n significantly contributing terms in the double sum, then $\mu=1$ in (6.43b). On the otherhand, for correlated signals (observed RF- incoherently here), Q_n is $O(n)$, and $\mu=2$. Examples of the former type are independently (incoherently observed and) generated pulsed carriers, such as those modelled in Secs. 20.3-(2), 20.4-3, [12], where each received signal element s_i is independent of the others, so that $\rho_{ij} = \delta_{ij}$ in effect, and $Q_n = 1$. For the latter type, we have coherent pulse trains (observed incoherently), where $\rho_{ij} = \cos \omega_0(t_i - t_j)$, cf. (5.13) (no doppler), for instance. Then Q_n^{-1} , (6.25), becomes $\frac{n}{2}[1+O(1/n)] \doteq \frac{n}{2}$, ($n \gg 1$), so that $\Pi_{\text{inc}}^{(*)} \sim n^2$. Intermediate values of μ , ($1 < \mu < 2$), arise when the received signals are partially decorrelated, as happens, for example, when there is carrier spreading (in frequency and therefore in time) because of randomly moving scatterers in the path of propagation, which generates a consequent doppler "smear" of the original signal waveform; Eq. (5.13), $\Delta\omega_d > 0$, shows a typical signal correlation function in the usual case of narrow-band signals subject to carrier doppler spread.

- (iii). The minimum detectable signal for coherent threshold detection, similarly, is ,

$$\langle a_0^2 \rangle_{\text{coh}}^{(*)} \sim n^{-1}, \text{ (cf. Tables 6.1a,b).} \quad (6.43c)$$

- (iv). The minimum detectable signal for incoherent threshold detection is, alternatively,

$$\langle a_0^2 \rangle_{\text{inc}}^{(*)} \sim n^{-\mu/2}, \quad (1 \leq \mu \leq 2), \text{ (cf. Tables 6.1a,b),} \quad (6.43d)$$

again depending on whether the received signal has an incoherent ($\mu=1$) to coherent structure ($\mu=2$), as determined, quantitatively by Q_n , cf. (6.25), (6.31), (6.36b), (6.41). Thus, note that it is possible for the minimum detectable signal in incoherent reception to behave like that for coherent reception, viz. $\langle a_0^2 \rangle \sim n^{-1}$, when $\mu=2$, i.e., when completely correlated signals can be used (and observed).

- (v). Maximum detectable signal range, $r_{\text{d-max}}^{(*)}$, whether for LOBD reception or the suboptimum correlation receivers, follows from (6.8) and (6.43c,d). We see at once that

$$r_{\text{d-max}}^{(*)} \Big|_{\text{coh}} \sim n^{1/2\gamma}; \quad r_{\text{d-max}}^{(*)} \Big|_{\text{inc}} \sim n^{\mu/4\gamma}, \quad 1 \leq \mu \leq 2. \quad (6.43e)$$

Thus, the larger the power law (γ), the larger must sample size (n) be to achieve a given maximum detectable range. Again, the coherent structure of the signal, if available and used, importantly aids the detection process and extends $r_{\text{d-max}}^{(*)}$.

- (vi). In the important limiting situation of gaussian noise our general results do indeed reduce to the earlier, "classical" results (cited in [12]). We have

(1). On-off Coherent Detection

$$\sigma_{o-coh}^2 = 2n\bar{a}_0^2, \text{ Eqs. (6.16), (6.17); } (L^{(2)}=1);$$

$$\text{Sec. 20.3-1; [12] : } \phi_{\bar{s}} = \sum_i \bar{s}_i^2 = 2n ;$$

$$\therefore \bar{a}_0^2 \phi_{\bar{s}} = 2n\bar{a}_0^2 = \sigma_{o-coh}^{(*)2}, \text{ in Eqs. (20.79), (20.120) of [12]}$$

\therefore Eqs. (6.3) are identical with Eq. (20.79), (20.120) of [12] when the noise is gaussian.

(2). On-off Incoherent Detection:

$$\sigma_{o-inc}^2 = \frac{1}{2} n \bar{a}_0^2 \quad (Q_n=1: \text{ incoherent signal structure})$$

$$L^{(4)}=2; L^{(2)}=1; \text{ from Eqs. (6.22)-(6.24); (6.35)}$$

$$\sigma_{o-inc} = \sqrt{\frac{n}{2}} \bar{a}_0 \text{ for instantaneous amplitudes; in Eqs. (6.3).}$$

When envelope detection with independent envelope signal samples is used, we have

$$\sigma_{o-inc}^2 |_{\text{envelope}} = n \bar{a}_0^2 ; \therefore \sigma_{o-inc} = \sqrt{n} \bar{a}_0 ,$$

and hence (20.131) of [12] agrees with (6.3). [Compare the envelope form of the threshold algorithm (20.128), [12], with (4.12) for amplitude cases.] With amplitude detection $\sigma_{o-inc} = \sqrt{n/2} \bar{a}_0$ in (6.3) gives precisely (20.91), [12], as required, where $\langle \phi_G \rangle = n$.

[(3). Equations (20.93, p. 876, [12], are incorrect in their factors 2, following the incorrect relation between ϕ_G and ϕ_{oG} in the footnote on p. 875, [12]. The correct relation is

$\Phi_G = \Phi_{OG}/2$, cf. (20.29a), [12], not $\Phi_G = 2\Phi_{OG}$. Thus, wherever Φ_{OG} appears in (20.93), divide by 4.]

(vii). Corrections:

Ref. [47]: Eq. (3.27), delete factor containing $L^{(4)}$; Eq. (3.27a), replace "2" by $\sqrt{2}$ in second factor of θ ; Eq. (3.28), rewrite as $\Phi_{inc}^* = \sigma_{o-inc}^*/\sqrt{2} = \sqrt{\Pi^*} \langle a_o^2 \rangle_{min-inc}^*$; Eq. (3.29), replace $2\theta_{inc}^*$ by Φ^* ; Eq. (3.30), replace argument of θ by $\sigma_{o-inc}^*/2\sqrt{2} = (1/2)\sqrt{\Pi_{inc}^*} a_o^2_{inc}^*$.

VI. Decibel Forms:

A convenient way of expressing our results in I-IV above is to use a decibel representation, so that factors are additive and powers are factors. This is particularly useful in numerical calculations where it is necessary to determine individual terms separately, initially before combining in the full relation. We have

$$\left\{ \begin{array}{l} \check{\sigma}_{o-coh}^{(*)2} = 0.3010 + \check{\Pi}_{coh}^{(*)} + \langle \check{a}_o^2 \rangle_{coh}^{(*)} \quad ; \quad \check{A} \equiv 10 \log_{10} A; \\ \check{\sigma}_{o-inc}^{(*)2} = 0.3010 + \check{\Pi}_{inc}^{(*)} + 2 \langle \check{a}_o^2 \rangle_{inc}^{(*)} . \end{array} \right. \quad (6.44a)$$

$$\left\{ \begin{array}{l} \check{\sigma}_{o-coh}^{(*)2} = 0.3010 + \check{\Pi}_{coh}^{(*)} + \langle \check{a}_o^2 \rangle_{coh}^{(*)} \quad ; \quad \check{A} \equiv 10 \log_{10} A; \\ \check{\sigma}_{o-inc}^{(*)2} = 0.3010 + \check{\Pi}_{inc}^{(*)} + 2 \langle \check{a}_o^2 \rangle_{inc}^{(*)} . \end{array} \right. \quad (6.44b)$$

Similarly, we get

$$\left\{ \begin{array}{l} \langle \check{a}_o^2 \rangle_{min-coh}^{(*)} = -\check{\Pi}_{coh}^{(*)} + 2[\check{C}_{N.P.}^{(*)} \text{ or } \check{C}_{I.O.}^{(*)}] , \\ \langle \check{a}_o^2 \rangle_{min-inc}^{(*)} = -\frac{1}{2} \check{\Pi}_{inc}^{(*)} + [\check{C}_{N.P.}^{(*)} \text{ or } \check{C}_{I.O.}^{(*)}] . \end{array} \right. \quad (6.45a)$$

$$\left\{ \begin{array}{l} \langle \check{a}_o^2 \rangle_{min-coh}^{(*)} = -\check{\Pi}_{coh}^{(*)} + 2[\check{C}_{N.P.}^{(*)} \text{ or } \check{C}_{I.O.}^{(*)}] , \\ \langle \check{a}_o^2 \rangle_{min-inc}^{(*)} = -\frac{1}{2} \check{\Pi}_{inc}^{(*)} + [\check{C}_{N.P.}^{(*)} \text{ or } \check{C}_{I.O.}^{(*)}] . \end{array} \right. \quad (6.45b)$$

(These relations hold for both the "on-off" and binary broad-band and narrow-band signal cases, of course.)

6.3 Performance Measures of Optimum vs. Suboptimum Threshold Reception:

Since performance, as measured by suitable probabilities of correct or incorrect decisions, $P_{D,e}^{(*)}$, can be expressed functionally for general input signals (broad- and narrow-band) by the general relation

$$P_{D,e}^{(*)} = F_{D,e}^{(*)}[\sigma_0^{(*)}] = \Pi^{(*)}(n) f(\langle a_0^2 \rangle_{\min}^{(*)}), \quad (6.46)$$

cf. (6.2), (6.4), etc., and (6.6), we have at least three principal ways of comparing performance, for the same signal waveforms against the same interference for the same mode of reception:

- $$\left\{ \begin{array}{l} \text{(I).} \quad \text{Given } n \text{ and } \langle a_0^2 \rangle_{\min} \text{ the same in both optimum and} \\ \quad \text{suboptimum cases, compare } P_{D,e} \text{ to } P_{D,e}^*; \\ \text{(II).} \quad \text{Given } P_{D,e} = P_{D,e}^*, \text{ same } n, \text{ compare } \langle a_0^2 \rangle_{\min} \text{ to } \langle a_0^2 \rangle_{\min}^*; \\ \text{(III).} \quad \text{Given } P_{D,e} = P_{D,e}^*, \text{ same input minimum detectable signals} \\ \quad (\langle a_0^2 \rangle_{\min} = \langle a_0^2 \rangle_{\min}^*), \text{ determine the increase in sample} \\ \quad \text{size } (n) \text{ of the suboptimum processor vis-à-vis that of} \\ \quad \text{the corresponding LOBD.} \end{array} \right. \quad (6.47a)$$

- $$\text{(Ia)-(IIIa): Same as (I)-(III), but for optimum coherent} \quad (6.47b) \\ \text{vs. optimum incoherent detection.}$$

The first comparison (I) gives a probability measure of the suboptimality of the suboptimum system compared to the optimum, for identical signal, noise, and observation conditions (period of observation is n and mode, e.g. coherent, incoherent, etc.). The second and third methods of comparison (II, III) require the same performance, but now with different input signal levels or sample sizes. Again, the noise conditions are unchanged in each instance, and the signal structure is unaltered, but the input signal level ($\langle a_0 \rangle$) or sample size may be changed.

Other modes of comparison are clearly possible. For example, for the same signals, sample sizes, modes of reception, we can compare performance for systems optimum in nongauss vs. those optimum in gauss. In fact, that is what we also do here, since the correlation detectors (with the correct biases) are themselves optimum in normal noise. A measure of superiority

of the proper processors in nongauss vis-à-vis gauss under these conditions is, of course, given by the degradation factor Φ_d^* , cf. (6.18), (6.38), (6.43), for example. Equivalently, we can measure this superiority by the extent to which $P_{D,e}^*$ are changed vis-à-vis $P_{D,e}$ (for the correlators), or performances can be compared based on different sample sizes. Still other possibilities arise, in the manner of Sec. 4.3 above, when algorithms optimal in one class of interference are used suboptimally against another class of noise. For the most part, we will consider the comparisons of (6.47a), as well as Φ_d^* directly.

Accordingly, from (6.47) we have

6.3.1 Comparisons, Eq. (6.47) Optimum vs. Suboptimum:

(I). Fixed Sample-Size (n) and Input Signals ($\langle a_0^2 \rangle_{\min}$):

From (6.18), (6.38),

$$\Phi_{d-}^*(n) \equiv (\Pi/\Pi^*)_{\text{coh/inc}}, \quad (\text{same } n = n^*),$$

we have directly the canonical relation

$$\sigma_0^2 = \Phi_d^* \sigma_0^{*2} \quad (6.48)$$

for both coherent and incoherent reception. This, in turn, in (6.2) gives directly, with

$$\sigma_0^* = \sqrt{2} [\theta^{-1} (2P_D^*/p-1) + A^*], \quad A^{(*)} \equiv \theta^{-1} (1 - 2\alpha_F^{(*)}), \quad (6.49)$$

on eliminating σ_0^* , the canonical form

$$P_D \cong \frac{p}{2} \{1 + \theta [\sqrt{\phi_d^*} \{ \theta^{-1} (2 \frac{P_D^*}{p} - 1) + \theta^{-1} (1 - 2\alpha_F^*) \} - \theta^{-1} (1 - 2\alpha_F)]\} \quad , \quad (6.50)$$

$$\cong \frac{p}{2} \{1 + \theta [\sqrt{\phi_d^*} C_{N.P.}^* - \theta^{-1} (1 - 2\alpha_F)]\} \quad , \quad (6.50a)$$

for both coherent and incoherent on-off or binary signal detection. With (6.50) we can compare P_D with P_D^* directly, where usually $\alpha_F^* = \alpha_F$. Clearly, since $0 \leq \phi_d^* \leq 1$, $P_D \leq P_D^*$ here, as expected.

Similarly, in the steady-state communication régime, where P_e^* is the more natural measure of performance once the desired signal has been initially established, we have from (6.48) in (6.5) for the symmetric channel ($\mu = 1$):

$$P_e \cong \frac{1}{2} \{1 - \theta [\sqrt{\phi_d^*} \theta^{-1} (1 - 2P_e^*)]\} \quad , \quad \theta^{-1} (1 - 2P_e^*) = \frac{1}{2} C_{I.O.}^* \quad , \quad (6.51)$$

where now, of course, $P_e \geq P_e^*$, ($\phi_d^* \leq 1$), as expected.

(II). Same Decision Probabilities ($P_{D,e} = P_{D,e}^*$), Sample Size (n):

Here the comparison is made between minimum detectable input signals when the decision probabilities [(6.2), (6.5), (6.6)] are equated. Thus, we have

$$P_{D,e} = P_{D,e}^* \quad ; \quad \therefore \quad \sigma_0 = \sigma_0^* \quad (6.52)$$

for all modes of operation here. From (6.9), (6.16), or (6.22b), (6.35), we get directly

$$\langle a_0^2 \rangle_{\text{min-coh}}^* = \Phi_{\text{d-coh}}^* \langle a_0^2 \rangle_{\text{min-coh}} ; \langle a_0^2 \rangle_{\text{min-inc}}^* = \sqrt{\Phi_{\text{d-inc}}^*} \langle a_0^2 \rangle_{\text{min-coh}}$$

(6.53)

which in db become

$$\langle a_0^2 \rangle_{\text{min-coh}}^* = \check{\Phi}_{\text{d-coh}}^* + \langle a_0^2 \rangle_{\text{min-coh}} ; \langle a_0^2 \rangle_{\text{min-inc}}^* = \frac{1}{2} \check{\Phi}_{\text{d-inc}}^* + \langle a_0^2 \rangle_{\text{min-inc}}$$

(6.53a)

all of which apply equally well for the on-off and binary cases, in form:
of course, the specific structure of Φ_{d}^* depends on whether or not "on-off"
or binary signals are employed, and the mode of reception, cf. Tables
6.1a,b.

(III). Same Decision Probabilities and Input Signals:

Here the input signal levels are the same, as are the probabilities of
decision, so that comparisons are naturally made in terms of sample size:
n vs. n*. This starts with $\sigma_0 = \sigma_0^*$, cf. (6.52), and using (6.9), (6.16),
and (6.22b), (6.35) we obtain now, with $\langle a_0^2 \rangle_{\text{min}} = \langle a_0^2 \rangle_{\text{min}}^*$:

$$\Pi^*(n^*) = \Pi(n)$$

(6.54)

generally, for coherent, incoherent, "on-off", binary signal reception,
etc. Applying (6.10), (6.17) specifically gives for both "on-off" and
binary operation:

(Opt. vs. Cross-correlator):

$$n_{\text{coh}}^* = \Phi_{\text{d-coh}}^* n_{\text{coh}} = n_{\text{coh}} / L^{(2)}$$

(6.55a)

for the simple correlator, and for the clipper correlator [cf. Sec. A.4-3 and Table 6.2]:

(opt. vs. clipper-correlators):

$$n_{\text{coh}}^* = \frac{4w_{1E}(0)^2 n_{\text{coh}}}{L_E^{(2)}} \quad (6.55b)$$

in these stationary régimes.

For the incoherent cases we obtain similarly, from (6.38), (6.40), (6.42), and Table 6.2, with Sec. (A.4-3), the more complex relations where n^* , n may appear implicitly, viz:

(opt. vs. auto-correlator):

$$(i). \text{ "on-off" } \quad \frac{n^*}{4} (L^{(4)} + 2L^{(2)})^2 [Q_{n^*} - 1] = \frac{nQ_n^2}{[(x^4 - 1) + 2(Q_n - 1)]} ; \quad (6.56a)$$

$$(ii). \text{ binary: } \left\{ \begin{array}{l} \underline{a_o^{(2)} \neq a_o^{(1)}}: \quad \frac{n^*}{4} (L^{(4)} + 2L^{(2)})^2 \{Q_{n^*}^{(21)} - 1\} = \frac{nQ_n^{(21)2}}{[x^4 - 1 + 2(Q_n^{(21)} - 1)]} , \quad (6.56b) \\ \underline{a_o^{(2)} = a_o^{(1)}}: \quad \frac{n^*}{4} L^{(2)2} \{Q_{n^*}^{(21)} - 1\} = \frac{n\{Q_n^{(21)} - 1\}^2}{[x^4 - 1 + 2(Q_n^{(21)} - 1)]} , \quad (6.56c) \end{array} \right.$$

cf. (6.30), (6.31), (6.33), (6.33a), (6.40), (6.41). Also, we have (6.24) vs. Table 6.2, and (6.30), (6.33), vs. Table 6.2 (binary) and Sec. (A.4-3):

(opt. vs. clipper correlator):

$$(i). \text{ "on-off" } \quad n^* [L_E^{(4)} + 2L_E^{(2)}]^2 (Q_{n^*} - 1) = \frac{n[-\sqrt{2} w_{1E}''(0) + 8w_{1E}(0)^2 Q_{n^*} - 1]^2}{2Q_n - 1} \quad (6.57a)$$

$$(ii). \text{ binary: } \left\{ \begin{array}{l} \underline{a_0^{(2)} \neq a_0^{(1)}}: \quad n^* [L_E^{(4)} + 2L_E^{(2)^2} \{Q_{n^*}^{(21)} - 1\}] \\ \\ = \frac{n[-\sqrt{2} w_{1E}''(0) + 8w_{1E}(0)^2 (Q_n^{(21)} - 1)]^2}{(2Q_n^{(21)} - 1)} \\ \\ \underline{a_0^{(2)} = a_0^{(1)}}: \quad \frac{n^* L_E^{(2)^2} \{Q_{n^*}^{(21)} - 1\}}{2} = 8n w_{1E}(0)^4 (Q_n^{(21)} - 1). \quad (6.57c) \end{array} \right.$$

The relationship between n^* and n in these incoherent cases is clearly not so straightforward as in the coherent cases (6.55), and depends noticeably on the degree of signal correlation, cf. remarks in V, Sec. 6.2 above.

6.3.2 Comparisons-Optimum Coherent vs. Optimum Incoherent Threshold Detection:

Just as we have compared optimum vs. suboptimum threshold detection algorithms in the same modes (i.e., coherent, incoherent) of reception in 6.3.1, (I)-(III) above, so also is it instructive to compare optimum threshold detection for these different modes. Thus, according to Eq. (6.47b) we repeat the comparisons of (6.47a), but now for coherent vs. incoherent detection, respectively. Accordingly, we have

(Ia). Fixed Sample-Size (n) and Same Input Signals

$$\underline{\langle a_0 \rangle_{\text{min-coh}}^* = \langle a_0 \rangle_{\text{min-inc}}^* :}$$

From (6.11b, 6.27a) with (6.9) and (6.22a) we can write directly

$$\begin{aligned} B_{\text{coh}}^* &= (\sigma_{\text{on-coh}}^*)^2 / 2 = \langle a_0^2 \rangle_{\text{min-coh}}^* \hat{a}_{\text{coh}} \Pi_{\text{coh}}^* ; \\ B_{\text{inc}}^* &= (\sigma_{\text{on-inc}}^*)^2 / 2 = (\langle a_0^2 \rangle_{\text{min-inc}}^*)^2 \hat{a}_{\text{inc}} \Pi_{\text{inc}}^* \end{aligned} \quad (6.48)'$$

so that we can define

$$\boxed{\Psi^* \equiv \hat{a}_{\text{inc}}^2 \Pi_{\text{inc}}^* / (\hat{a}_{\text{coh}} \Pi_{\text{inc}}^*)^2} \quad (6.49)'$$

where

$$\hat{a}_{\text{coh}} \equiv \frac{\sum_i^n (\bar{a}_{oi} \bar{s}_i)^2 / 2n \bar{a}_0^2 + \bar{a}_0^2 / \bar{a}_0^2}{\bar{a}_0^2} \equiv 1 - \eta \text{ (stat. cases);} \quad (6.49a)'$$

$$0 \leq \eta \equiv \text{var } a_0 / \bar{a}_0^2 (<1) ;$$

$$\hat{a}_{\text{inc}} \equiv \left(\frac{\sum_i^n \langle a_{oi}^2 s_i^2 \rangle^2 / n \bar{a}_0^2}{\bar{a}_0^2} \right)^{1/2} \rightarrow 1 \text{ (stat. cases),} \quad (6.49b)'$$

since $\bar{s}_i^2 = 1$.

Here η represents the "fading factor" whose anatomy is examined in somewhat more detail in II, Sec.7.1 ff. Therefore, we have directly (in these stationary cases)

$$\Psi^* = L^{(4)} \left[1 + \frac{2L^{(2)^2}}{L^{(4)}} (Q_n - 1) \right] / 8(1 - \eta)^2 n L^{(2)^2} , \quad (6.50)'$$

and

$$B_{\text{inc}}^* = \Psi^* (B_{\text{coh}}^*)^2 , \quad [\text{cf. (6.11) - (6.11b)}] \quad (6.51)'$$

Using (6.48)', (6.49)' in (6.2), (6.5), and (6.27) enables us to write these probability measures of performance respectively as

$$P_{\text{D-inc}}^* \approx \frac{p}{2} \{ 1 + \theta [\sqrt{\Psi^*} \{ \theta^{-1} (2p_{\text{D-coh}}^* - 1) + \theta^{-1} (1 - 2\alpha_F^*) \}^2 - \theta^{-1} (1 - 2\alpha_F^*)] \} ; \quad \alpha_F^* = (\alpha_F^*)_{\text{coh}} ; \quad (6.52)'$$

$$P_{\text{e-inc}}^* \approx \frac{1}{2} \{ 1 - \theta [2\sqrt{\Psi^*} \theta^{-1} (1 - 2p_{\text{e-coh}}^*)^2] \} ; \quad (p = q = \frac{1}{2}) . \quad (6.53)'$$

Alternatively, we can express P_{coh}^* in terms of P_{inc}^* :

$$P_{\text{D-coh}}^* \approx \frac{p}{2} \{ 1 + \theta [(\Psi^*)^{1/4} \{ \theta^{-1} (2p_{\text{D-inc}}^* - 1) + \theta^{-1} (1 - 2\alpha_F^*) \}^{1/2} - \theta^{-1} (1 - 2\alpha_F^*)] \} ; \quad \alpha_F^* = (\alpha_F^*)_{\text{coh}} \quad (6.54)'$$

$$P_{e\text{-coh}}^* \approx \frac{1}{2} \left\{ 1 - \Theta \left[\frac{(\Psi^*)^{1/4}}{\sqrt{2}} \Theta^{-1} (1 - 2P_{e\text{-inc}}^*)^{1/2} \right] \right\} ; \quad (p = q = \frac{1}{2}) , \quad (6.55)'$$

where Ψ^* in the common stationary cases is given by (6.50)' above.

(IIa). Same Decision Probabilities and Sample Size:

In this case we may expect different values of the respective (minimum) input signal (-to-noise ratios). Thus (6.52) is modified to

$$P_{D,e\text{-coh}}^* = P_{D,e\text{-inc}}^* ; \quad \dots \quad \sigma_{o\text{-coh}}^* = \sigma_{o\text{-inc}}^* ; \quad \dots \quad B_{\text{coh}}^* = B_{\text{inc}}^* ; \quad n_{\text{coh}}^* = n_{\text{inc}}^* \quad (6.56)'$$

so that from (6.48)' it follows directly that

$$\left\langle a_0^2 \right\rangle_{\text{inc}}^* = \left(\hat{a}_{\text{coh}}^* \hat{\Pi}_{\text{coh}}^* / \hat{a}_{\text{inc}}^* \hat{\Pi}_{\text{inc}}^* \right)^{1/2} \sqrt{\left\langle a_0^2 \right\rangle_{\text{coh}}^*} ,$$

$$\left[\left\langle a_0^2 \right\rangle_{\text{coh}}^* = \left\langle a_0^2 \right\rangle_{\text{inc}}^* , \text{ etc.} \right] , \quad (6.57a)$$

$$= \left\{ \frac{8(1-\eta)L^{(2)}}{L^{(4)} + 2L^{(2)2} (Q_n - 1)} \right\}^{1/2} \sqrt{\left\langle a_0^2 \right\rangle_{\text{coh}}^*} . \quad (6.57b)'$$

In the case of coherent signal waveforms (large n), we have [cf. (A.2-42e)]

$$Q_n \doteq \frac{n}{2} \text{ (slow fading)} ; \quad Q_n \doteq \frac{n}{2} (1-\eta)^2 \text{ (rapid fading)} \quad (6.58)'$$

and since $L^{(4)} = O(2L^{(2)2})$ in the highly nongaussian situations [cf.

Figs. 7.7, 7.8 (Class A), and Figs. 7.11, 7.12 (Class B)], we see that (6.57)' reduces to

$$\left\langle a_0^2 \right\rangle_{\text{inc-slow}}^* \approx \sqrt{\frac{8(1-\eta)}{nL^{(2)}}} \left(\left\langle a_0^2 \right\rangle_{\text{coh}}^* \right)^{1/2} , \quad (6.59a)'$$

$$\left\langle a_0^2 \right\rangle_{\text{inc-fast}}^* \approx \sqrt{\frac{8}{nL^{(2)}(1-\eta)}} \left(\left\langle a_0^2 \right\rangle_{\text{coh}}^* \right)^{1/2} , \quad (6.59b)'$$

respectively for slow and rapid fading.

(IIIa). Same Decision Probabilities and Input Signals:

For this case, the comparison is between processing gains, or in more detail, between sample sizes n_{coh}^* , n_{inc}^* , needed to achieve the same performance in the two modes of threshold detection, when the minimum detectable signals are required to be the same. Accordingly, from (6.48)' again we have now

$$\hat{a}_{\text{coh}}^{\Pi^*} = \left\langle a_0^2 \right\rangle_{\text{coh}}^* \hat{a}_{\text{inc}}^{\Pi^*}, \text{ or } B_{\text{coh}}^* = (\Psi^*)^{-1}, \text{ cf. (6.51)'} \quad (6.60)'$$

Since $\left\langle a_0^2 \right\rangle_{\text{coh}}^* = B_{\text{coh}}^* / \hat{a}_{\text{coh}}^{\Pi^*}$, cf. (6.48)', we get finally

$$n_{\text{coh}}^* = \frac{1}{L(2)} \left\{ n_{\text{inc}}^* B_{\text{coh}}^* \left[L^{(4)} + 2L^{(2)^2} \binom{Q}{n^* - \text{inc}} \right] \right. \\ \left. / 8(1 - \eta)^2 \right\}^{1/2}. \quad (6.61)'$$

With slow or rapid fading and coherent signal waveforms ($n \gg 1$), as before, cf. (6.53)', (6.61)' reduces to

$$n_{\text{coh-slow}}^* \approx n_{\text{inc}}^* \sqrt{B_{\text{coh}}^*} / 2\sqrt{2}(1 - \eta); \quad n_{\text{coh-fast}}^* \approx n_{\text{inc}}^* \sqrt{B_{\text{coh}}^* / 8}. \quad (6.62)'$$

(We note that slow fading works to the relative disadvantage of coherent vis-à-vis incoherent detection.)

6.3.3 Asymptotic Relative Efficiencies:

It is a comparatively simple matter now to determine another frequently used measure of performance, namely, the Asymptotic Relative Efficiency (ARE), (for example, see [14], p. 242, Eqs. (78b, 80).) This is defined for nonzero signal ($\theta > 0$) and the same decision (i.e. probability) controls [$C_{\text{N.P.}}$, $C_{\text{I.O.}}$, etc., cf. (6.11b) etc.], as the limit as sample sizes become infinite, of the ratio of the normalized "distances" of the two receiver characteristics under comparison when the same input signals are employed, in the same noise backgrounds. Thus, for receiver 1 vs. receiver 2 we have (in the "on-off" cases):

$$\begin{aligned} \text{ARE} \Big|_{\text{"on-off"}, \theta > 0} &= \lim_{n_1, n_2 \rightarrow \infty} \left\{ \frac{\langle g^{(1)} \rangle_1 - \langle g^{(1)} \rangle_0}{\hat{\sigma}_0^{(1)}} \Big/ \left(\frac{\langle g^{(2)} \rangle_1 - \langle g^{(2)} \rangle_0}{\hat{\sigma}_0^{(2)}} \right) \right\} \\ &= \lim_{n_1, n_2 \rightarrow \infty} \{ \sigma_0^{(1)} / \sigma_0^{(2)} \}, \end{aligned} \quad (6.58)$$

where $\sigma_0^{(1)}, (2)$ are defined in (A.4-12), (A.4-13) [(A.4-72), (A.4-74) also] for general (most of the time) suboptimum systems, where $\hat{\sigma}_0^{(1)}, (2)$ are the respective variances of the receiver algorithms $g^{(1)}, g^{(2)}$ under H_0 , cf. (A.4-9), (A.4-29); (A.4-71), (A.4-73). For binary signals (6.58) becomes directly

$$\text{ARE} \Big|_{\text{binary}, \theta > 0} = \lim_{n_1, n_2 \rightarrow \infty} \left\{ \frac{\sigma_{01}^{(21)}}{\sigma_{02}^{(21)}} \right\}. \quad (6.58a)$$

Applying the general relation (6.6) in its canonical form (6.48) here to (6.58), we see at once that the ARE for comparison against the optimum detector become simply

$$\text{ARE}^* \Big|_{\theta > 0} \equiv \lim_{n, n^* \rightarrow \infty} \left(\frac{\sigma_0}{\sigma^*} \right) = \lim_{n, n^* \rightarrow \infty} \sqrt{\phi_{d-}^{(*)}} \quad (\leq 1), \quad (6.59)$$

for "on-off" and binary signalling. In the case of suboptimum system comparisons (6.59) becomes

$$\text{ARE}_{1/2} \Big|_{\theta > 0} = \lim_{n_1, n_2 \rightarrow \infty} \frac{1}{\phi_{d-}^{*2}} = \lim_{n_1, n_2 \rightarrow \infty} \frac{\sigma_0^{(1)}}{\sigma_0^{(2)}} \quad (\leq 1), \quad (6.59a)$$

where systems 1, 2 are so chosen that this limiting ratio is always equal to or less than unity. (Of course, if systems 1 and 2 are both optimum, the ARE is unity.)[†] Again, we remark that narrow-band as well as broad-band signal types are included canonically here.

From the text above (cf. Tables 6.1a,b, 6.2) we easily establish the following useful examples:

I. Coherent Reception:

- (i). simple correlator:
optimum
- (ii). clipper correlator:
optimum
- (iii). simple correlator:
clipper correlator

$$\begin{aligned} \text{ARE}_{\text{coh}}^* &= \sqrt{1/L^{(2)}} \ (\leq 1); & \text{["on-off"; binary]} & \quad (6.60a) \\ \text{ARE}_{\text{coh}}^* &= \sqrt{4w_{1E}(0)^2/L^{(2)}} \ (\leq 1); & \text{["on-off"; binary]} & \quad (6.60b) \\ \text{ARE}_{(1/2)\text{coh}} &= 1/4w_{1E}(0) \ (\leq 1); & \text{["on-off", binary]} & \quad (6.60c) \end{aligned}$$

II. Incoherent Reception:

- (i). simple-correlator:
optimum

$$\begin{aligned} \text{ARE}_{\text{inc}}^* \Big|_{\text{on-off}} &= \lim_{n \rightarrow \infty} \left\{ \frac{4Q_n^2}{(L^{(4)} + 2L^{(2)})^2 \{Q_n - 1\}} \right. \\ &\quad \left. \cdot \frac{1}{(x^4 - 1 + 2\{Q_n - 1\})^2} \right\}^{1/2}, \text{ cf. Eq. (6.38);} & (6.61a) \\ \left. \begin{array}{l} \frac{a^{(1)} \neq a^{(2)}}{\text{---} \circ \text{---} \circ \text{---}} \\ \frac{a^{(1)} = a^{(2)}}{\text{---} \circ \text{---} \circ \text{---}} \end{array} \right\} \text{ARE}_{\text{inc}}^* \Big|_{\text{binary}} &= \lim_{n \rightarrow \infty} \left\{ \frac{4Q_n^{(21)2}}{(L^{(4)} + 2L^{(2)})^2 \{Q_n^{(21)} - 1\}} \right. \\ &\quad \left. \cdot \frac{1}{(x^4 - 1 + 2\{Q_n^{(21)} - 1\})^2} \right\}^{1/2}, \text{ cf. Eq. (6.42a)} & (6.61b) \\ \text{ARE}_{\text{inc}}^* \Big|_{\text{binary}} &= \lim_{n \rightarrow \infty} \left\{ \frac{2(\hat{Q}_n^{(21)} - 1)}{L^{(2)^2 [x^4 - 1 + 2(\hat{Q}_n^{(21)} - 1)]} \right\}^{1/2}, & (6.61c) \\ &\text{cf. Eq. (6.42b).} & \end{aligned}$$

[†]Note, however, that ARE = 1 does not necessarily mean both algorithms are optimum, cf. last ¶ of III.

(ii). clipper-correlator
optimum

$$\text{ARE}_{\text{inc}}^* \Big|_{\text{on-off}} = \lim_{n \rightarrow \infty} \left(\frac{[-\sqrt{2} w_{1E}''(0) + 8w_{1E}(0)^2 \{Q_n - 1\}]^2}{(2Q_n - 1)[L_E^{(4)} + 2L_E^{(2)}]^2 \{Q_n - 1\}} \right)^{\frac{1}{2}} ; \quad (6.62a)$$

$$\frac{a^{(1)} \neq a^{(2)}}{a_0}: \text{ARE}_{\text{inc}}^* \Big|_{\text{binary}} = \lim_{n \rightarrow \infty} \left(\frac{[-\sqrt{2} w_{1E}''(0) + 8w_{1E}(0)^2 \{Q_n^{(21)} - 1\}]^2}{(2Q_n^{(21)} - 1)[L_E^{(4)} + 2L_E^{(2)}]^2 \{Q_n^{(21)} - 1\}} \right)^{\frac{1}{2}} ; \quad (6.62b)$$

$$\frac{a^{(1)} = a^{(2)}}{a_0}: \text{ARE}_{\text{inc}}^* \Big|_{\text{binary}} = (4w_{1E}(0)^2 / L_E^{(2)})^2 ; \quad (6.62c)$$

Here the signal factors $Q_n, Q_n^{(21)}, \hat{Q}_n^{(21)}$, are defined specifically by

"on-off": $Q_n \equiv 1 + \frac{1}{n} \sum_{ij} m_{ij}^2 \rho_{ij}^2$; cf. Eq. (6.25); $m_{ij} \equiv \overline{a_{oi} a_{oj}} / a_0^2$;

$$\rho_{ij} = \langle s_i s_j \rangle ; \quad (6.63a)$$

$$\frac{a^{(1)} \neq a^{(2)}}{a_0}: Q_n^{(21)} = \frac{\sum_{ij} \{ \langle a_0^{(2)} \rangle^2 m_{ij}^{(2)} \rho_{ij}^{(2s)} - \langle a_0^{(1)} \rangle^2 m_{ij}^{(1)} \rho_{ij}^{(1s)} \}^2}{n \{ \langle a_0^{(2)} \rangle^2 - \langle a_0^{(1)} \rangle^2 \}^2} ;$$

Eq. (6.31); (6.63b)

$$\frac{a^{(1)} = a^{(2)}}{a_0}: \hat{Q}_n^{(21)} = 1 + \frac{1}{n} \sum_{ij} m_{ij}^2 (\rho_{ij}^{(2s)} - \rho_{ij}^{(1s)})^2 ; \text{ Eq. (6.33) } . \quad (6.63c)$$

The noise parameters are $L^{(2)} = \langle \ell^2 \rangle$, $L^{(4)} = \langle (\ell^2 + \ell'^2) \rangle_0$, cf. (A.1-15, 19b), as before.

We have also the comparison of suboptimums here, cf. (6.60c):

(iii). simple-correlator
clipper correlator:

$$\begin{aligned}
 \text{ARE}_{\text{inc}} \Big|_{\text{on-off}} &= \lim_{n \rightarrow \infty} \left(\frac{4Q_n^2 \{2Q_n - 1\}}{[x^4 - 1 + 2(Q_n - 1)] [-\sqrt{2}w_{1E}(0)]^4 + 8w_{1E}(0)^2 \{Q_n - 1\}} \right)^{\frac{1}{2}} \\
 &= \text{Eq. (6.61a)} / \text{Eq. (6.62a)}; \quad (6.64a) \\
 \frac{a_o^{(1)} \neq a_o^{(2)}}{a_o^{(1)} = a_o^{(2)}}: \text{ARE}_{\text{inc}} \Big|_{\text{binary}} &= \lim_{n \rightarrow \infty} \left(\frac{4Q_n^{(21)2} \{2Q_n^{(21)} - 1\}}{[x^4 - 1 + 2(Q_n^{(21)} - 1)] [-\sqrt{2}w_{1E}(0)]^4 + 8w_{1E}(0)^2 \{Q_n^{(21)} - 1\}} \right)^{\frac{1}{2}} \\
 &= \text{Eq. (6.61b)} / \text{Eq. (6.62b)} \quad (6.64b)
 \end{aligned}$$

$$\begin{aligned}
 \frac{a_o^{(1)} = a_o^{(2)}}{a_o^{(1)} \neq a_o^{(2)}}: \text{ARE}_{\text{inc}} \Big|_{\text{binary}} &= \lim_{n \rightarrow \infty} \left(\frac{(\hat{Q}_n^{(21)} - 1)}{8[x^4 - 1 + 2(\hat{Q}_n^{(21)} - 1)] w_{1E}(0)^4} \right)^{\frac{1}{2}} \\
 &= \text{Eq. (6.61c)} / \text{Eq. (6.62c)}. \quad (6.64c)
 \end{aligned}$$

(We remember that when the clipper correlator is optimum, i.e. when the noise is Laplace noise, cf. Sec. A.4-3, we must use the optimum forms $L_{F:E} \rightarrow L_E$, etc., cf. (A.4-39)-(A.4-46), where $\hat{L}^{(4)} \rightarrow L^{(4)} \rightarrow L_E^{(4)}$, etc., so that in the incoherent cases specifically the $\text{ARE}^* = 1$, as required.)

As some simple examples, let us consider coherent reception (for general signals) when (1), the noise is gaussian, and (2), when it is LaPlacian, e.g.:

$$w_{1E}(x)_{\text{gauss}} = \frac{e^{-x^2/2}}{\sqrt{2\pi}} ; \left\{ \begin{array}{l} L_E^{(2)}=1; \overline{x^2}=1; \\ \text{Eq. (A.1-22)}. \end{array} \right. \quad (6.65a)$$

$$w_{1E}(x)_{\text{Laplace}} = \frac{1}{\sqrt{2}} e^{-|x|\sqrt{2}} ; \left\{ \begin{array}{l} L_E^{(2)}=2; (\overline{x^2}=1). \\ \text{Eq. (A.4-65a)}. \end{array} \right. \quad (6.65b)$$

We have at once from (6.65) into (6.60) the simple results

$$(i). \quad \frac{\text{simple correlator}}{\text{opt.}} : \text{ARE}_{\text{coh}}^* \Big|_{\text{gauss}} = 1; \text{ARE}_{\text{coh}}^* \Big|_{\text{Laplace}} = 1/\sqrt{2} \quad (6.66a)$$

$$(ii). \quad \frac{\text{clipper correlator}}{\text{opt.}} : \text{ARE}_{\text{coh}}^* \Big|_{\text{gauss}} = \sqrt{\frac{2}{\pi}}; \text{ARE}_{\text{coh}}^* \Big|_{\text{Laplace}} = 1; \quad (6.66b)$$

$$(iii). \quad \left(\frac{\text{simple correlator}}{\text{clipper correlator}} \right)^{-1} : \text{ARE}_{\text{coh}}^* \Big|_{\text{gauss}} = \sqrt{\frac{2}{\pi}} ; \frac{\text{simple correl.}}{\text{clipper correl.}} \Big|_{\text{Laplace}} = \frac{1}{\sqrt{2}}. \quad (6.66c)$$

Equation (6.66) shows that there is not much difference 0(<.2db) between simple and clipper correlators in these threshold cases when they operate in gaussian and Laplace noise, to which they are respectively optimum. However, when the usual Class A or B interference is the principal noise mechanism, the simple correlators (although optimum in gauss) have been found to be very suboptimum here 0(20-40db or more), [13], whereas the superclipper correlators (at least in the coherent régimes) remain only slightly degraded 0(1.0 dB) from the proper optimum processor [42], [45].

We recall from Sec. 6.3, V above, that depending on the coherence of the signal during the data acquisition period (0,T), the signal factors Q_n , etc., cf. (6.63), are $0(n^\mu)$, $0 \leq \mu \leq 1$. Thus, for incoherent reception and signals made comparatively incoherent (by combinations of rapid fading and doppler or by the mode of observation: independent signal samples,

for example), we have $\mu=0$, i.e. Q_∞ is essentially independent of n , and then the results (6.61)-(6.64) remain unchanged. However, when the signal remains highly correlated during the observation period, $Q_\infty \rightarrow 0 (n \rightarrow \infty)$, and (6.61)-(6.64) reduce to the somewhat simpler forms:

III. Incoherent Reception; Coherent Signals:

$$(i). \quad \frac{\text{simple correlator}}{\text{optimum}}: \quad ARE_{inc}^* = 1/L^{(2)} \quad ; \quad (\text{on-off and binary}) \quad (6.67a)$$

$$(ii). \quad \frac{\text{clipper correlator}}{\text{optimum}}: \quad ARE_{inc}^* = [4w_{1E}(0)^2/L^{(2)}] \quad ; \quad (\text{on-off and binary}); \quad (6.67b)$$

$$(iii). \quad \frac{\text{simple correlator}}{\text{clipper correlator}}: \quad ARE_{inc} = [1/4w_{1E}(0)^2] \quad ; \quad (\text{on-off and binary}). \quad (6.67d)$$

Comparing these results (6.67) for the incoherent cases with those for the coherent situations (6.60), we see that the ARE's for the former are just the square of the ARE's for the latter in their respective comparisons, when the desired signals are fully coherent in structure and are so observed. On the other hand, when this coherent signal structure is partially or totally destroyed, the corresponding ARE's, Eqs. (6.61)-(6.64), are further reduced, as we would expect. We also observe that signal level symmetry $[a_0^{(1)} = a_0^{(2)}]$ considerably simplifies the result, cf. (6.61c), (6.62c), (6.64c), vis-à-vis the asymmetric cases $[a_0^{(1)} \neq a_0^{(2)}]$, including the "on-off" situation. The ARE's for coherent reception are larger (and sometimes much larger) than their incoherent counterparts: (6.60) vs. (6.67).

Finally, we remark that although the ARE's, like output signal-to-noise ratios $(\sigma_0^{(*)})^2$, (6.6), processing gains $(\Pi^{()})$, and minimum detectable signals $(\langle a_0^2 \rangle_{\min})$, are useful measures of receiver performance and performance comparisons, they are not directly (or linearly) related to actual performance, as measured by the appropriate decision probabilities (P_D , P_e , etc.). Furthermore, the ARE's are limiting forms ($n \rightarrow \infty$), whereas in practice one deals with finite n ($\gg 1$).

Moreover, closely related to the essentially second-moment character of the ARE's (cf. 6.58)), is the fact that they can be ambiguous measures of performance. This may be demonstrated, for example, in the case of coherent threshold detection, Sec. 6.2, I, II, where for the suboptimum detector we choose the optimum form (4.1), but without the bias, $\hat{B}_{n\text{-coh}}^*$. Thus, $\sigma_0^2 = \sigma_0^{*2}$, $(\langle g \rangle_1 - \langle g \rangle_0)^{(*)} = \sigma_0^{*2}$, so that the ARE = 1. This says that on the basis of the ARE the two algorithms are equivalent. But $\langle g \rangle_1 = \sigma_0^{*2} + \log \mu$, $\langle g \rangle_0 = \log \mu$, so that (2.32) becomes $(\mu=1) P_e \doteq \frac{1}{2} [1 - \frac{1}{2} \theta(\sigma_0^*/\sqrt{2})]$ which is to be compared with $P_e^* \doteq \frac{1}{2} [1 - \theta(\sigma_0^*/2\sqrt{2})]$. Since $\theta(x/2) < \frac{1}{2} \theta(x)$, $x > 0$, clearly $P_e > P_e^*$ in this example. In fact, $P_e \doteq 1/4$ for the usually large σ_0^* . Thus, on the basis of the more comprehensive probability measures, the algorithm without the (correct) bias can be clearly inferior. Furthermore, this suboptimum algorithm is not asymptotically optimum (AO), since it is $(\mu=1) G(\sigma_0^{*2}, 0; \sigma_0^{*2})$, under H_0, H_1 , which does not obey the n.+s. conditions (A.3-8,9).

For all these reasons, then, these latter quantities (i.e., P_D^* , etc.) are the more complete and unambiguous descriptors of performance and are ultimately to be preferred to the ARE's when receiver performance is to be assessed and compared under the practical constraint of finite sample size ($1 \ll n \ll \infty$), not only for the threshold conditions postulated here, but for all input signal levels.

6.4 Input Signal Conditions for (Optimum) Threshold Algorithms and Performance

There are two conditions on the maximum level of the input signal $a_0^2 (>0)$ which must be obeyed[†] if the detection algorithms g_n^* are to remain not only LOBD's but AODA's as well (as sample size becomes larger).

As we have already noted (cf. Sec. 2.4, Secs. A.2-1,2,3,4, etc.), the first condition is to insure that $\text{var}_{1,\theta} g_n^* \doteq \text{var}_{0,0} g_n^*$, cf. (2.29), (A.2-14), (A.2-40), (A.2-50b), which in turn is required for asymptotic optimality (AO), cf. (Appendix) Section A.3-3, as well as consistency of the test (detection) as $n \rightarrow \infty$ and for providing the associated proper bias, \hat{B}_n^* .

[†]In the limiting case of continuous sampling on the observation interval! we shall discuss this point and its relation to the discrete sampling cases of our current analysis in Sec. 6.4 III, following.

The second condition stems from the fact that the coherent LOBD is a truncated expansion of $\log \Lambda_n$, which omits the "incoherent" term $O(\theta^2)$, so that it is possible in some nongaussian noise situations that, mathematically, incoherent LOBD's perform better than coherent LOBD's. Of course, physically this appears to be a contradiction[†]: coherent detection should always be at least no worse than incoherent detection under otherwise the same conditions, since the former employs the additional relevant information about the signal phase (or epoch). Consequently, there can also be an upper limit on input signal level (a_0^2) beyond which the truncation [i.e., omission of the incoherent terms, $O(\theta^2)$] of the coherent algorithm leads to this contradiction in performance, and hence beyond which the associated performance measures are not used.

Of course, the algorithms themselves are employable at all signal levels ($0 < a_0^2$), but are no longer optimal as a_0^2 is increased outside the lesser of the two limits indicated. Their performance must then be re-evaluated: if $n \gg 1$, the Central Limit Theorem still applies, but $\sigma_{1n}^{*2} \neq \sigma_{0n}^{*2}$, i.e., $\text{var}_{1,0} g_n^* \neq \text{var}_{0,0} g_n^*$, and it is then possible for "coherent" detection by these now suboptimum algorithms to be inferior to the corresponding "incoherent" detectors.

I. "On-off" Detection:

Let us look further at the "second condition" noted above: viz., from (6.2), (6.5) (as well as (6.5a), (6.5e) in the binary signal cases):

(Opt.) Coherent Det $>$ (Opt.) Incoherent Det:

$$\sigma_{0\text{-coh}}^* \geq \sigma_{0\text{-inc}}^*$$

(large n).

(6.68a)

This insures (for sufficiently large n, where (6.2) etc. apply) that (optimum) coherent performance is never worse than (optimum) incoherent performance under otherwise the same conditions. For the "on-off" cases

[†] See footnote, page 102.

from (6.9) and (6.22b) we can write (6.68a) as

$$\sqrt{\Pi_{\text{coh}}^* \langle a_0^2 \rangle_{\text{min-coh}}^*} \geq \sqrt{\Pi_{\text{inc}}^* \langle a_0^2 \rangle_{\text{min-inc}}^*}, \quad (6.68b)$$

and, using (6.10), (6.24) we get at once

$$\langle a_0^2 \rangle_{\text{min-coh}}^* \geq \frac{\Pi_{\text{inc}}^*}{\Pi_{\text{coh}}^*} \langle a_0^2 \rangle_{\text{min-inc}}^{*2} = \left\{ \frac{L^{(4)} + 2L^{(2)^2} (Q_n - 1)}{8L^{(2)}} \right\} \langle a_0^2 \rangle_{\text{min-inc}}^{*2}. \quad (6.68c)$$

Equation (6.68c) is to be used in conjunction with the first condition (on a_0^2), i.e., that $\text{var}_{1, \theta} g_n^* = \text{var}_{0,0} g_n^*$, here (A.2-15a), which is specifically in the stationary noise régime:

Eq. (A.2-15a): coherent:

$$\langle a_0^2 \rangle_{\text{min-coh}}^* \ll x_0^* \equiv \frac{L^{(2)} \sum_i \hat{a}_{oi}^2 \bar{s}_i^2}{\left| \sum_i \bar{s}_i^2 \hat{a}_{oi}^2 \left[\frac{L^{(2,2)}}{2} \left(\frac{\bar{a}_{oi}^2}{a_0^2} \right) - L^{(2)^2} \hat{a}_{oi}^2 \right] + L^{(2)^2} \sum_{ij} (\hat{a}_{oi} \hat{a}_{oj} (m_{ij} - \hat{a}_{oi} \hat{a}_{oj}) \bar{s}_i \bar{s}_j) \right|} \quad (6.69)$$

$$\hat{a}_{oi} \equiv \bar{a}_{oi} / \sqrt{a_0^2} \quad ; \quad (6.69a)$$

Eq. (A.2-42): incoherent:

$$\langle a_0^2 \rangle_{\text{min-inc}}^* \ll y_0^* \equiv \frac{L^{(4)} + 2L^{(2)^2} (Q_n - 1)}{\left| \frac{L^{(6)}}{2} + 6L^{(2)} L^{(2,2)} Q_n + L^{(2)^3} R_n \right|} \quad (6.70)$$

In the important special cases of slow and no fading ($\bar{a}_{oi} = a_0, \bar{a}_{oi}^2 = a_0^2$;

$\therefore m_{ij} = 1$), or rapid fading ($\overline{a_{oi} a_{oj}} = \overline{a_{oi}} \overline{a_{oj}}$), Eq. (6.69) simplifies directly to

$$x_0^* = \frac{L^{(2)}}{|L^{(2,2)}/2 - (1-\eta)L^{(2)2}|} = \frac{\langle \ell^2 \rangle_0}{\text{var}_0 \ell^2} \quad (6.71)$$

Similarly, with incoherent signal structures (A.2-42b), or totally coherent signal structures (A.2-42f), we have

$$\text{(Incoherent structure): } y_0^* = \frac{L^{(4)}}{|L^{(6)}/2 + 6L^{(2)}L^{(2,2)}|} ;$$

$$\text{(coherent structure): } y_0^* = \frac{L^{(2)}}{3L^{(2,2)} + 2L^{(2)2}} , \quad (Q_n \doteq n/2; R_n \doteq 2n) , \quad (6.72)$$

where we take the maximum value of F_n^{-1} in (A.2-42f), for the strictest condition on $0 < a_0^2 \ll 1$. [Some numerical values of (x_0^*, y_0^*) are shown in Figs. 7.20-7.22 ff.]

Then, as the second condition, (6.68c) is used to set additional upper bounds on the input signal (var_0^2). Letting

$$x \equiv \langle a_0^2 \rangle_{\text{min-coh}}^* ; y \equiv \langle a_0^2 \rangle_{\text{min-inc}}^* ; \Pi^* \equiv \Pi_{\text{inc}}^* / \Pi_{\text{coh}}^* , \quad (6.73)$$

we have for (6.68c)

$$\text{2nd condition: } \boxed{x \geq \Pi^* y^2} ; \text{ with: 1st. condition: } \begin{cases} x \ll x_0^*, \text{ Eqs. (6.69), (6.71)} \\ y \ll y_0^*, \text{ Eqs. (6.70), (6.72)} \end{cases}$$

$$(6.74)$$

The points $y=x$, or $1/\pi^* \geq x = y$, which at $(1/\pi^*)$ or below the curve $x = \pi^*y^2$, and which are within the region of individual constraints on (x,y) , e.g., the dotted lines in Fig. 6.1, are all permissible values of $\langle a_0^2 \rangle_{\text{min-coh,inc}}^*$. The curves $y^2\pi^* = x$ represent the limiting condition $P_{\text{e-coh}}^* = P_{\text{e-inc}}^*$, or $P_{\text{D-coh}}^* = P_{\text{D-inc}}^*$. When we require coherent and incoherent performance to be equal, i.e. when we specify the limiting probabilities ($P_{\text{D-coh}}^* = P_{\text{D-inc}}^*$, etc.) which we can accept, that portion of the parabola $x = \pi^*y^2$ which lies within the rectangle $(x,y) [\ll (x_0, y_0)]$ determines the acceptable values of $\langle a_0^2 \rangle_{\text{min-coh,inc}}^*$.

Accordingly, to use the various relations in Section 6.1-6.3 to obtain minimum detectable signal (or maximum range, cf. [34]), when either a purely coherent or incoherent threshold detection algorithm is employed, we calculate the appropriate quantities, cf. (6.74), for both the coherent and incoherent régimes, in order to obtain physically acceptable results, even though we may be interested in only one or the other mode of detection. Thus, we may proceed as follows for minimum detectable signals (in these stationary cases):

A. Minimum Detectable Signals:

- (1). Calculate $\langle a_0^2 \rangle_{\text{min-coh}}^*$ from (6.11) for coherent reception;
- (2). Calculate $\langle a_0^2 \rangle_{\text{min-inc}}^*$ from (6.27) for incoherent detection;
- (3). Use (6.69) or (6.71) for x_0 ; (6.70), or (6.72) for y_0 , to determine the coherent/incoherent conditions for equal threshold variances;
- (4). Compute $x = \pi^*y^2$, (6.74), for the various $\langle a_0^2 \rangle_{\text{min}}^*$ and locate the results of (1), (2) within the region $x \geq \pi^*y^2$, cf. Fig. 6.1. Physically acceptable results here are (usually) those for which the calculated values fall within the bounded (i.e. shaded) region [but see remarks in III ff.].

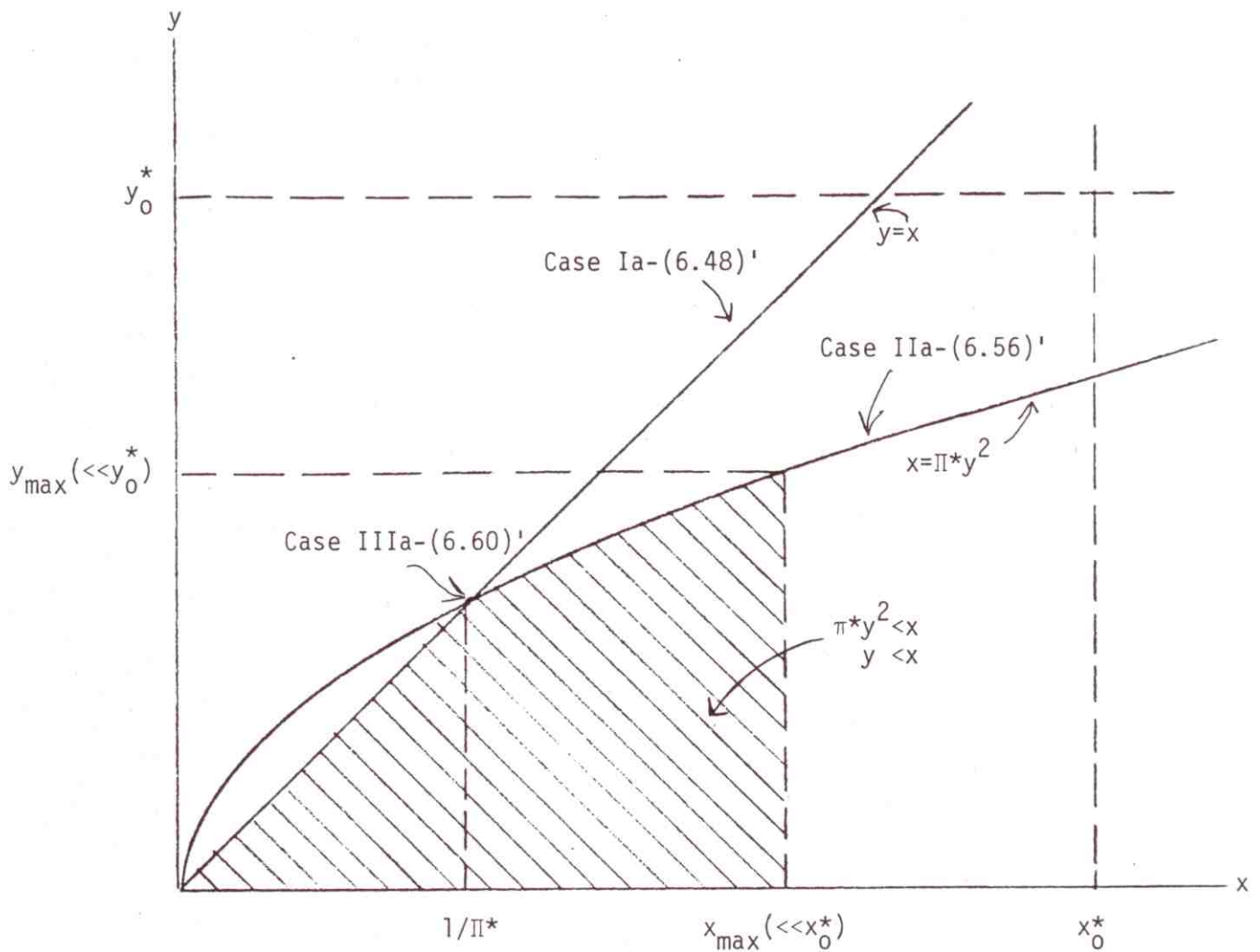


Figure 6.1. Sketch of the relationship between $x \left(= \langle a_0^2 \rangle_{\text{min-coh}}^* \right)$ and $y \left(= \langle a_0^2 \rangle_{\text{min-inc}}^* \right)$, showing the domain (shaded) wherein "coherent reception" \geq "incoherent reception," for physical applications (same sample size, n).

II. Binary Signal Detection:

The same considerations apply for optimum binary signal reception as above for the cases of "on-off" detection, e.g., in addition to the condition of equality of variances ($\text{var}_{1,\theta} g_n^{(21)*} = \text{var}_{0,\theta} g_n^{(21)*}$) we must satisfy (6.68a) as well. Here, of course, we replace Π_{coh}^* by $\Pi_{\text{coh}}^{(21)*}$, etc., $\langle a_o^2 \rangle_{\text{min}}^*$ by $\langle a_o^2 \rangle^{(21)*}$, etc., and Q_n by $Q_n^{(21)}$ in (6.68b,c), where specifically we employ (6.12), (6.13), (6.29)-(6.31). The first "small-signal" (or equal variance) conditions, analogous to (6.69) etc., are now given (in the stationary régimes) by

Eq. (A.2-50a) :
(coherent)

$$\left\{ \begin{array}{l} \langle a_o^2 \rangle_{\text{min-coh}}^{(21)*} \ll x_o^{(21)*} \\ \text{Eq. (6.14)} \end{array} \right. \equiv \frac{L^{(2)} \left(\sum_i^n \langle \Delta\theta_i \rangle^2 \right)^2}{\left| \sum_i \langle \Delta\theta_i \rangle^2 \left\{ \langle (a_{oi}^{(2)}, (1))^2 \rangle_{L^{(2,2)}} / 2 - \left(\langle a_{oi}^{(2)}, (1) \rangle \right)^2_{L^{(2)} \right\}} \right. \\ \left. + L^{(2)2} \sum_{ij} \langle \Delta\theta_i \rangle \langle \Delta\theta_j \rangle \cdot (\bar{s}_i \cdot \bar{s}_j)^{(2),(1)} \frac{1}{\{ a_{oi}^{(2)} a_{oj}^{(2)} \}^{(2),(1)}} \right. \\ \left. - [\langle a_{oi} \rangle \langle a_{oj} \rangle]^{(2),(1)} \right|, \quad (6.75)$$

$$\langle \Delta\theta_i \rangle \equiv \langle a_{oi}^{(2)} s_i^{(2)} \rangle - \langle a_{oi}^{(1)} s_i^{(1)} \rangle, \quad (6.75a)$$

cf. (6.69), (6.69a), and

Eq. (A.2-57):
(incoherent):

$$\left\{ \begin{array}{l} \langle a_0^2 \rangle_{\text{min-inc}}^{(21)*} \ll y_0^{(21)*} \\ \text{Eq. (6.69)} \end{array} \right. \equiv \frac{L^{(4)} + 2L^{(2)^2} (Q_n^{(21)})_{-1}}{\left| \frac{L^{(6)}}{2} + 6L^{(2)} L^{(2,2)} Q_n^{(21)} + L^{(2)^3} R_n^{(21)} \right|}, \quad (6.76)$$

(Eq. A.2-59) ,

for slow or no fading and stationary noise, in which $Q_n^{(21)}$, $R_n^{(21)}$ are given by (A.2-60a,b) explicitly.

For the important special cases of signals with no fading, in symmetrical channels, we have (A.2-50e) for $x_0^{(21)*}$, viz.

$$\text{[no fading; sym.]: } x_0^{(21)*} = \frac{L^{(2)} \sum_i (\bar{s}_i^{(2)} - \bar{s}_i^{(1)})^2}{\left| \{ L^{(2,2)}/2 - L^{(2)^2} \} \sum_i (\bar{s}_i^{(2)} - \bar{s}_i^{(1)})^2 \bar{s}_i^{(2), (1)} \right|}, \quad (6.77)$$

and from (A.2-62), for both coherent and incoherent signal structures

$$y_0^{(21)*} \equiv \frac{L^{(4)}}{\left| L^{(6)}/2 + 6L^{(2)} L^{(2,2)} \right|}, \quad (6.78)$$

cf. (6.71), (6.72) above. Still other forms can be obtained from (6.75), (6.76), depending on channel conditions. In any case, (6.73), (6.74) apply generally, with $x_0^* \rightarrow x_0^{(21)*}$, etc., now. The domain of input signal levels for applicability of the optimum algorithms is likewise sketched in Fig. 6.1, where, of course, $x = \langle a_0^{(2)^2} \rangle_{\text{min-coh}}^*$ or $\langle a_0^{(1)^2} \rangle_{\text{min-coh}}^*$, etc.: there are thus a pair of (x,y)'s now, when $a_0^{(2)} \neq a_0^{(1)}$, but only a single set (x,y) when the channel is symmetrical: $a_0^{(2)} = a_0^{(1)} = a_0$. The general procedure for determining minimum detectable signals is again given by A. above, suitably modified, e.g.:

A. Minimum Detectable Signals:

- (1). Calculate $\langle a_0^2 \rangle_{\text{min-coh}}^{(21)*}$, from (6.14);
- (2). Calculate $\langle a_0^2 \rangle_{\text{min-inc}}^{(21)*}$ from (6.29); (or 6.33);
- (3). Use (6.75) or (6.77) for x_0^* ; (6.76) or (6.78) for y_0^* , (e.g., the equal variance conditions on both coherent and incoherent reception;
- (4). Compute $x = \pi^{(21)*} y^2$, (6.74), $\pi^* \rightarrow \pi^{(21)*}$, where $\pi^{(21)*} = \pi_{\text{inc}}^{(21)*} / \pi_{\text{coh}}^{(21)*}$, cf. (6.13), (6.30).

III. The Second Input Signal Condition -- Optimum Incoherent vs. Coherent Detection: Discussion

Our starting point is Figure 6.1. For the moment let us impose the "coherent-vs-incoherent" condition posited in (6.68a) above, here, of course, for discrete sampling such that the noise samples are statistically independent--our universal condition in this study, cf. Sec. 2.4 et seq.

Then, we can make the following observations about Figure 6.1:

- (i) The parabola (6.74) is the contour of Case IIa, Eq. (6.56)' et seq., for optimum incoherent threshold performance being equal to optimum coherent performance.
- (ii) The straight line ($y=x$) embodies Case Ia, Eq. (6.48)' et seq., where coherent performance is better (i.e., smaller error probabilities) than incoherent performance, with the same sample sizes, when $\langle a_0^2 \rangle_{\text{min-coh}}^* (\equiv x) = y \equiv \langle a_0^2 \rangle_{\text{min-inc}}^* \leq 1/\pi^*$. For $x=y$ larger than $x_{\text{III}} = y_{\text{III}} = 1/\pi^*$ coherent performance is inferior to incoherent performance.
- (iii) At $x=y=1/\pi^* = x_{\text{III}} = y_{\text{III}}$ we have Case IIIa, (6.60)' et seq., where $n_{\text{inc}}^* > n_{\text{coh}}^*$ ($\gg 1$) usually.
- (iv) Here x_0^* , y_0^* are bounding values obtained from the basic Condition I, namely the "equal variance" condition which is necessary to insure asymptotic optimality at small but non-vanishing signals.

(Explicit examples relating x_0^* , y_0^* to the associated minimum detectable signal $\langle a_0^2 \rangle_{\text{min}}^*$ are given by Eqs. (6.69)-(6.72) above.) If x_{max} , y_{max} are the largest input signal values permitted, the allowed minimum detectable

signals (x,y) must obey the inequalities $x \leq x_{\max} \ll x_0^*$ or $y \leq y_{\max} \ll y_0^*$. Here the usual quantitative choice of the inequality (\ll) is 13 dB or 15 dB in practice. (Of course, the value given to " \ll " is arbitrary, dependent on a reasonable choice of what is meant by "small" signals.) Accordingly, the rectangular (shaded) region bounded by x_{\max}, y_{\max} in Figure 6.1 is the domain wherein the A0, or equal-variance condition holds practically.

Now, from Figure 6.1 it is clear that it may be possible for these threshold algorithms to be A0 (as well as LOB) and have coherent detection with larger minimum detectable signals, or larger error probabilities (inferior performance), or both, than (A0) incoherent detection. When this happens, we call the region of (x,y) values an anomalous region, with respect to the conditions $\langle a_0^2 \rangle_{\min\text{-coh}}^* \leq \langle a_0^2 \rangle_{\min\text{-inc}}^*$, and coherent performance \geq incoherent performance. Thus, in the region formed by $y=x$ and the parabola (within x_{\max}, y_{\max}) we have the "anomalous" situation $y > x$, with incoherent performance better than coherent. The region bounded by the line $y=x$, the parabola, x_{\max} , and $y=0$ is the non-anomalous region, as shown in Figure 6.1.

The results of Figure 6.1 show that for both optimum coherent and incoherent threshold detectors which are A0 (as well as LOB) one can have any combination of minimum detectable signal and performance inequalities for the same data sample size. This, in turn, means that the so-called Condition II, defined by Eq. (6.74) is not (for discrete, independent noise samples) an ultimate constraint on the validity of "practical" optimality: we can disregard Condition II as long as Condition I--the equal variance condition--is obeyed. Thus, there is ultimately only Condition I, which sets a bound on the largest value of input minimum detectable signal for which the A0 still obtains (cf. Appendix A3). Moreover, we may expect Condition II to be automatically satisfied in the limit of continuous sampling. The formal use of Condition II in the discrete case, however, is helpful in identifying the apparently anomalous regions of behavior. Of course, with continuous sampling only the "regular" region is occupied, because then coherent detection cannot be any less effective than incoherent detection for otherwise the same conditions of operation.

This follows in as much as more signal information (i.e., epoch) is used in the coherent cases than in incoherent reception, while all the noise data, viz. those contained in the n-th order pdf's $w_n(x)_N$ as $n \rightarrow \infty$, are employed in either observation mode. [We note that the derivatives of $w_n(x)_N$, as $n \rightarrow \infty$, contain no additional noise information.]

The explanation for the anomalous behavior of the optimum incoherent vis-à-vis the optimum coherent detector lies in the different effective amount of relevant signal and noise information available under independent (noise) samples. Although all signal (i.e., waveform) information is used in both detection modes, with only the epoch information lacking in the incoherent cases[†], more relevant noise information is available in the incoherent cases. This is apparent from the fact that for coherent detection we require $\ell (= \frac{d}{dx} \log w_n(x))$ in the algorithm and $L^{(2)} (\equiv \langle \ell^2 \rangle_0)$ in the performance measure, whereas both ℓ and ℓ' are needed in the incoherent algorithm, and $L^{(4)} (\equiv \langle (\ell^2 + \ell')^2 \rangle_0)$ as well as $L^{(2)}$, in its performance. In addition, there is further information embodied in the way $L^{(2)}$ and $L^{(4)}$ appear in σ_{0-inc}^* , along with their combination with signal structure (Q_n), cf. (6.24); for example, the functional form of Π_{inc}^* , as well as its individual $L^{(2)}$, $L^{(4)}$, and Q_n components.

Whether or not the use of this added information is enough to offset the loss of epoch information in the signal will depend, of course, on the specific nature of the nongaussian noise, signal structure, the signal's interaction with the noise, and on the probability controls (P_D^* , α_F^* , etc.) under which the receiver is set to operate. For signals which maintain their structure (e.g., no doppler smearing) we may have "anomalous" behavior, i.e., the incoherent minimum detectable signals are smaller than for the corresponding

[†] For simplicity, we confine the argument to the important limiting cases where total waveform information is available to the receiver. This, however, is not a restriction on our general argument. We note, also, that with proper choice of epoch and sampling intervals in the coherent cases, discrete signal sampling is fully equivalent to continuous signal sampling on the observation interval (O.T.).

coherent cases (under the same performance measures). On the other hand, incoherent reception of "incoherent" signals is always inferior (in the sense of larger minimum detectable signals for the same controls) to coherent reception of coherent waveforms, as we would expect. Specific examples of these behaviors are presented in Sec. 7.4 ff. Finally, even in the gauss noise cases ($L^{(2)}=1$, $L^{(4)}=2$) we may expect anomalous behavior for the same reasons. [An academic exception is the case of the completely known signal, for the reasons cited in Sec. A.3-6, I, esp. p. A66.] The general magnitude of the anomalies in $\langle a_0^2 \rangle_{\min}^*$ appears to be 0(2-3 dB), cf. Sec. 7.4 ff. All our comments here apply equally to the earlier results Sec. 5.1, V, [34].

IV . Remarks on Suboptimum Receivers:

Similar conditions on the largest "small-signal" inputs to suboptimum receivers, giving equal variances under H_0 , H_1 , etc. are derived in Appendix A.4, cf. (A.4-10) for the coherent cases and (A.4-30) for the incoherent detectors, generally. In the case of simple correlators these equal variance conditions are given by (A.4-59), and for energy detectors, by (A.4-63), while for hard-limiting or "super-clipper" correlators, these conditions are given in (A.4-70). For binary signals, see the remarks in Sec. A.4-4.

However, when these receivers are suboptimum [as they will be in most instances unless they are operating in the noise for which they are "matched," i.e., become optimum, viz., gauss noise (A.4-50a) for the simple correlators, "Laplace noise" (A.4-50b) for the hard-limiter correlators], there is no reason to assume that coherent reception will necessarily always be better than incoherent reception for otherwise the same reception conditions. Such a situation will depend on the detectors themselves vis-à-vis noise and signal. Consequently, we do not impose the second condition, cf. Eqs. (6.68), on the magnitude of the input signal, so that only the conditions on equal variances referenced above are needed in the evaluation of performance using the (suboptimum) results of Section 6.1, etc.

Of course, these suboptimum algorithms can be used at all input signal levels, but then $\text{var}_{1,\theta} g \neq \text{var}_{0,0} g$ and the large-sample ($n \gg 1$) expressions for P_D , P_e , etc., cf. Sec. 6.1, must be appropriately modified, along the lines of (2.23)-(2.27), cf. (2.26), (2.27) specifically.

6.5 The Composite LOBD:

We have shown (in Appendix A.3-6) that the composite LOBD, \bar{g} , which includes both coherent ($\bar{\theta} \geq 0$) and incoherent processing ($\bar{\theta}^2 > 0$, $\bar{\theta} = 0$), is also an AODA, and in the "on-off" cases is given explicitly by

$$\begin{aligned}
 g_{n\text{-comp}}^* &= \log \mu + \hat{B}_{\text{comp}}^* + \frac{1}{2} \sum_{ij}^n [-2L_i \langle \theta_i \rangle \delta_{ij} + (L_i L_j + L_i^2 \delta_{ij}) \langle \theta_i \theta_j \rangle] \\
 &= \log \mu + \text{LOBD}_{\text{coh}} + \text{LOBD}_{\text{inc}},
 \end{aligned}
 \tag{6.79a}$$

where the bias is

$$\begin{aligned}
 \hat{B}_{n\text{-comp}}^* &= -\frac{1}{8} \sum_{ij}^n \{ 4L_i^{(2)} \langle \theta_i \rangle^2 \delta_{ij} + \langle \theta_i \theta_j \rangle^2 [(L_i^{(4)} - 2L_i^{(2)^2}) \delta_{ij} + 2L_i^{(2)} L_j^{(2)}] \} \\
 &= \hat{B}_{n\text{-coh}}^* + \hat{B}_{n\text{-inc}}^*,
 \end{aligned}
 \tag{6.79b}$$

and the variance $\sigma_{\text{on-comp}}^{*2}$ ($= \text{var}_{0,0} g_{n\text{-comp}}^*$) is given by

$$\begin{aligned}
 \sigma_{\text{on-comp}}^{*2} &= \frac{1}{4} \sum_{ij}^n \{ 4L_i^{(2)} \langle \theta_i \rangle^2 \delta_{ij} + \langle \theta_i \theta_j \rangle^2 [(L_i^{(4)} - 2L_i^{(2)^2}) \delta_{ij} + 2L_i^{(2)} L_j^{(2)}] \} \\
 &= \sigma_{\text{on-coh}}^{*2} + \sigma_{\text{on-inc}}^{*2}.
 \end{aligned}
 \tag{6.79c}$$

The equal-variance, or "small-signal" condition that $\sigma_{1n}^{*2} = \sigma_{\text{on}}^{*2}$ here is given by (6.69) or (6.70), whichever is the stricter. Note that there

is here no "second-condition", cf. Sec. 6.4, I, II above, since there is now no question of a purely coherent processor in possible competition with an incoherent algorithm to produce possibly inferior performance vis-à-vis the incoherent algorithm: there is just a single, albeit composite algorithm.

Performance, as measured by the probabilities P_D^* , or P_e^* , cf. (6.2) - (6.5), follows at once on applying $\sigma_{\text{on-comp}}^*$ therein: (cf. Footnote p. 55).

With binary signals [cf. II, Appendix A.3-6] we have the extensions of (6.79), viz:

$$\begin{aligned}
 g_{\text{n-comp}}^{(21)*} = & \log \mu + \hat{B}_{\text{n-comp}}^{(21)*} + \frac{1}{2} \sum_{ij}^n \{-2L_i [\langle a_{oi}^{(2)} s_i^{(2)} \rangle - \langle a_{oi}^{(1)} s_i^{(1)} \rangle] \delta_{ij} \\
 & + [L_i L_j + L_i^2 \delta_{ij}] [\langle a_{oi} a_{oj} s_i s_j \rangle^{(2)} - \langle a_{oi} a_{oj} s_i s_j \rangle^{(1)}] \}, \quad (6.80)
 \end{aligned}$$

in which the bias and associated variance $\sigma_{\text{on-comp}}^{(21)*2}$ are specifically

$$\begin{aligned}
 \hat{B}_{\text{n-comp}}^{(21)*} = & -\frac{1}{8} \sum_{ij}^n [4L_i^{(2)} \{\langle a_{oi}^{(2)} s_i^{(2)} \rangle^2 - \langle a_{oi}^{(1)} s_i^{(1)} \rangle^2\} \delta_{ij} \\
 & + [\langle a_{oi}^{(2)} a_{oj}^{(2)} s_i^{(2)} s_j^{(2)} \rangle^2 - \langle a_{oi}^{(1)} a_{oj}^{(1)} s_i^{(1)} s_j^{(1)} \rangle^2] \\
 & \cdot [(L_i^{(4)} - 2L_i^{(2)})^2 \delta_{ij} + 2L_i^{(2)} L_j^{(2)}] \}, \quad (6.80a) \\
 = & \hat{B}_{\text{n-coh}}^{(21)*} + \hat{B}_{\text{n-inc}}^{(21)*}
 \end{aligned}$$